7. D. J. Evans, *J. Stat. Phys.*, **22**, 81 (1980).
8. W. G. Hoover, D. J. Evans, R. B. Hickman, A. J. C. Ladd, W. T. Ashurst, and B. Moran, *Phys. Rev.*, **A22**, 1690 (1980).
9. D. J. Evans and H. J. M. Hanley, *Physica* **103A**, 343 (1980).
10. D. J. Evans, *Phys. Rev.*, **A23**, 1988 (1981).
11. D. J. Evans, *Molec. Phys.*, **42**, 1355 (1981).
12. D. J. Evans, *Phys. Lett.*, **A91**, 457 (1982).
13. D. J. Evans, W. G. Hoover, B. H. Failor, B. Moran, and A. J. C. Ladd, *Phys. Rev.*, **A28**, 1016 (1983).
14. M. J. Gillan and M. Dixon, *J. Phys.*, **C16**, 869 (1983).
15. D. J. Evans, *J. Chem. Phys.*, **78**, 3297 (1983).
16. D. J. Evans, *Physica* **118A**, 51 (1983).
17. D. J. Evans and G. P. Morris, *Chem. Phys.*, **77**, 63 (1983).
18. D. J. Evans and G. P. Morris, *Phys. Rev.*, **A30**, 1528 (1984).
19. A. D. Simmons and P. H. Cummings, *Chem. Phys. Lett.*, **129**, 92 (1986).
20. D. J. Evans, *Phys. Rev.* **A34**, 1449 (1986).
21. P. T. Cummings and G. P. Morris, *J. Phys. F: Met. Phys.*, **17**, 593 (1987).
22. P. T. Cummings and G. P. Morris, *J. Phys. F: Met. Phys.*, **18**, 1439 (1988).
23. P. T. Cummings and T. L. Varner, *J. Chem. Phys.*, **89**, 6391 (1988).
24. D. J. Evans and G. P. Morris, *Comput. Phys. Rep.*, **1**, 297 (1984).
25. G. Ciccotti, G. Jacucci and I. R. McDonald, *J. Stat. Phys.*, **21**, 1 (1979).
26. G. P. Morriss and D. J. Evans, *Molec. Phys.*, **54**, 135 (1985).
27. K. F. Gauss, *J. Reine Angew. Math.*, **IV**, 232 (1829).
28. A. W. Lees and S. F. Edwards, *J. Phys.*, **C5**, 1921 (1972).
29. W. C. Gear, 'Numerical Initial Value Problems in Ordinary Differential Equations' (McGraw-Hill, New York, 1965).
30. S. H. Lee and P. J. Rossky, in "Proceedings of the 10 th Korean Scientists and Engineers Conference" (Inchen, Korea, 1987), Physical science part, p. 150.
31. A. Rahman, *Phys. Rev.*, **136A**, 405 (1964).
32. S. H. Kuo, "Computer Applications of Numerical Methods" (Addison-Wesley, Philippines, 1972), p. 244.
33. G. A. Cook, "Argon, Helium and the Rare Gases" (Intersciences, NY, 1961).

Non-equilibrium Molecular Dynamics Simulations of Thermal Transport Coefficients of Liquid Water

Song Hi Lee*, Gyeong Keun Moon, and Sang Gu Choi†

Department of Chemistry, Kyungsung University, Pusan 608-736.
†Department of Industrial Safety, Yang San Junior College, Yangsan 626-800. *Received January 29, 1991*

In a recent paper[1] we reported equilibrium (EMD) and non-equilibrium (NEMD) molecular dynamics simulations of liquid argon using the Green-Kubo relations and NEMD algorithms to calculate the thermal transport coefficients-the self-diffusion coefficient, shear viscosity, and thermal conductivity. The overall agreement with experimental data is quite good. In this paper the same technique is applied to calculate the thermal transport coefficients of liquid water at 298.15 K and 1 atm using TIP4P model for the interaction between water molecules. The EMD results show difficulty to apply the Green-Kubo relations since the time-correlation functions of liquid water are oscillating and not decaying rapidly enough except the velocity auto-correlation function. The NEMD results are found to be within approximately ±30~40% error bars, which makes it possible to apply the NEMD technique to other molecular liquids.

Introduction

In recent years, the non-equilibrium molecular dynamics (NEMD) simulations have emerged as a powerful tool for the study of thermal transport coefficients - self-diffusion coefficient, shear and bulk viscosities, and thermal conductivity-of both simple and molecular fluids. Recent development include the sllod algorithm[2,3] for shear viscosity, the color current technique[4] for self-diffusion coefficient, the Evans algorithm[5,6] for thermal conductivity, and the use of Gauss's principle[4,7] of least constraint for isokinetic and/or isobaric ensemble simulations. More recently a homogeneous NEMD simulation[8] to investigate the nature of liquid surfur under extreme shear using the potential model developed by Stillinger and Weber[9] which involves three-body interaction is reported. Furthermore the principle of the color current algorithm is applied to non-equilibrium Brownian dynamics (NEBD) simulations,[10] in which the non-equilibrium state is achived by including a constant electric field in the Smoluchowski dynamics, to calculate the self-diffusion coefficients of the ions in a model electrolyte solutions.

In a recent paper[1] we reported equilibrium molecular dynamics (Green-Kubo relations[11]) and non-equilibrium molecular dynamics simulations of liquid argon at 94.4 K and 1 atm to determine the thermal transport coefficients. The overall agreement of the EMD and NEMD results is quite good in comparison with experimental data. This means that the Green-Kubo relations and the NEMD algorithms are re-

liable for the calculation of the thermal transport coefficients of simple liquid which is modeled by the usual Lennard-Jones potential. Here we report a continuation of the earlier work on equlibrium and non-equilibrium molecular dynamics applied to determine the thermal transport coefficients of liquid water at 298.15 K and 1 atm. This research is motivated by the need to test the validity of the NEMD and EMD (Green-Kubo relations) techniques in calculation of the thermal transport coefficients of a molecular liquid. The chosen model potential for liquid water is the TIP4P potential which is described in Sec. III. (4).

The outline of the paper is as follow: In Sec. II the Green-Kubo relations, relations between time correlation functions and thermal transport coefficients, are introduced. In Sec. III the NEMD algorithm and equation of motions, including Gauss's principle of least constraint for constant translational and rotational temperatures, are briefly described. The NEMD results for the thermal transport coefficients of liquid water are compared with those obtained from the EMD simulations and experimental data in Sec. IV. Finally in Sec. V concluding remarks are presented.

Time-Correlation Function and Green-Kubo Relations

Correlations between two different quantities A and B are measured in the usual statistical sense, by means of the correlation coefficient C_{AB}

$$C_{AB}=\langle \delta A \delta B\rangle/\sigma(A)\sigma(B) \tag{1}$$

where $\sigma^2(A)=\langle \delta A^2\rangle=\langle A^2\rangle-\langle A\rangle^2$ and $\delta A=A-\langle A\rangle$ with the notation of ensemble average, $\langle\cdots\rangle$. Schwartz inequalities guarantee that the absolute value of C_{AB} lies between 0 and 1, with values close to 1 indicating a high degree of correlation. The idea of the correlation coefficient may be extended in a very useful way, by considering A and B to be evaluated at two different times. The resulting quantity is a function of the time difference t: it is a 'time-correlation functrion' $C_{AB}(t)$. For identical functions, $C_{AA}(t)$ is called an autocorrelation function and its time integral (from $t=0$ to $t=\infty$) is a correlation time τ_A. These functions are of great interest in computer simulation: (a) they give a clear picture of the dynamics in a fluid; (b) their time integrals τ_A may be related directly to macroscopic transport coefficients (Green-Kubo relations); (c) their Fourier transforms $\tilde{C}_{AA}(\omega)$ may often be related to experimental spectra. The non-normalized correlation function is defined

$$C_{AB}(t)=\langle \delta A(t)\delta B(0)\rangle=\langle \delta A[\Gamma(t)]\delta B[\Gamma(0)]\rangle \tag{2}$$

where we use the abbreviation Γ for a particular point in phase space, so that

$$C_{AB}(t)=C_{AB}(t)/\sigma(A)\sigma(B) \tag{3}$$

or

$$C_{AA}(t)=C_{AA}(t)/\sigma^2(A)=C_{AA}(t)/C_{AA}(0) \tag{4}$$

Just like $\langle \delta A\delta B\rangle$, $C_{AB}(t)$ is different for different ensembles. The computation of $C_{AB}(t)$ may be thought of as a two-stage process. First, we must select initial state points $\Gamma(0)$, according to the desired distribution $f_{ens}(\Gamma)$, over which we will subsequently average. Second, we must evaluate $\Gamma(t)$. This means solving the true (Newtonian) equations of motion. By this means, time-dependent properties may be calculated in any ensemble. In practice, the mechanical equations of motion are almost always used for both purpose, i.e. we use molecular dynamics to calculate time-correlation functions in the canonical ensemble.

Transport coefficients are defined in terms of the response of a system to a pertubation. For example, the diffusion coefficient relates the particle flux to a concentration gradient, while the shear viscosity is a measure of the shear stress induced by an applied velocity gradient. By introducing such pertubations in to the Hamiltonian, or directly into the equations of motion, their effect on the distribution function f_{ens} may be calculated. Generally a time-dependent non-equilibrium distribution $f(t)=f_{ens}+\delta f(t)$ is produced. Hence, any non-equilibrium ensemble average (in particular, the desired response) may be calculated. By retaining the linear terms in the pertubation, and comparing the equation for the response with a macroscopic transport equation, we may identify the transport coefficient. This is usually the infinite time integral of an equilibrium time-correlation function of the form

$$\beta=\int_0^\infty dt\langle \dot{A}(t)\dot{A}(0)\rangle \tag{4}$$

where β is the transport coefficient and A is a variable appearing in the pertubation term in the Hamiltonian. Associated with any expression of this kind, there is also an 'Einstein relation'

$$2t\beta=\langle [A(t)-A(0)]^2\rangle \tag{5}$$

which holds at large t (compared with the correlation time of A). The connection between Eqs. (4) and (5) may easily be established by integration by parts. Note that only a few genuine transport coefficients exist, *i.e.*, for only a few 'hydrodynamic' variables A do Eqs. (4) and (5) give a non-zero β.

The self-diffusion coefficient D_s is given (in three dimensions) by

$$D_s=\frac{1}{3}\int_0^\infty dt\langle v_i(t)\cdot v_i(0)\rangle \tag{6}$$

where $v_i(t)$ is the center-of-mass velocity of a single molecule. The corresponding Einstein relation, valid at long times, is

$$2tD_s=\frac{1}{3}\langle |r_i(t)-r_i(0)|^2\rangle \tag{7}$$

where $r_i(t)$ is the molecular position. In practice, these averages would be computed for each of the N particles in the simulation, the results added together, and divided by N, to improve statistical accuracy.

The shear viscosity η is given by

$$\eta=\frac{V}{kT}\int_0^\infty dt\langle P_{xy}(t)P_{xy}(0)\rangle \tag{8}$$

or

$$2t\eta=\frac{V}{kT}\langle [Q_{xy}(t)-Q_{xy}(0)]^2\rangle \tag{9}$$

where

$$P_{xy}=\frac{1}{V}\left[\sum_i mv_{ix}v_{iy}+\sum_i r_{ix}f_{iy}\right] \tag{10}$$

is an off-diagonal ($x\neq y$) element of the pressure tensor and

$$Q_{xy}=\frac{1}{V}\sum_i mr_{ix}v_{iy} \tag{11}$$

The negative of P_{xy} is often called the stress tensor. These quantities are multi-particle properties, properties of the system as a whole, and so no additional averaging over the N particles is possible. Consequently η is subject to much greater statistical imprecision than D_s.

The thermal conductivity λ can be written as

$$\lambda=\frac{V}{kT^2}\int_o^\infty \mathrm{d}t\langle J_{Qx}(t)J_{Qx}(0)\rangle \tag{12}$$

or

$$2t\lambda=\frac{V}{kT^2}\langle[S_x(t)-S_x(0)]^2\rangle \tag{13}$$

where J_{Qx} is a component of the energy current

$$J_{Qx}=\frac{1}{V}\left[\sum_i E_i v_{ix}+\frac{1}{2}\sum_i\sum_j r_{ijx}(v_i\cdot F_{ij})\right] \tag{14}$$

which is the time derivative of

$$S_x=\frac{1}{V}\sum_i r_{ix}(E_i-\bar{E}) \tag{15}$$

The term $\sum_i r_{ix}\bar{E}$ makes no contribution if $\sum_i r_{ix}=0$, as is the case in a normal one-component molecular dynamics simulation. In calculating the energy of each molecule E_i, the potential energy of two molecules (assuming pairwise potentials) is taken to be divided equally between them:

$$E_i=\frac{mv_i^2}{2}+\frac{1}{2}\sum_i\sum_j V(r_{ij}) \tag{16}$$

Eqs. (6), (8), and (12) are the so-called Green-Kubo reations for the self-diffusion coefficient, shear viscosity, and thermal conductivity, respectively.

Nonequilbrium Molecular Dynamics

The Color Current Technique for Self-diffusion Coefficient. Consider the perturbating color field $F(t)$ at time 0 applied to the Hamiltonian H_0 with color charges c_i:

$$H=H_0+\sum_i c_i x_i F(t),\quad t>0 \tag{17}$$

For simplicity c_i is given by $(-1)^i$ for an even number of particles N. The response of the color current density J to the applied color field $F(t)$ is

$$J_x=\frac{1}{V}\sum_i c_i\dot{x}_i \tag{18}$$

The linear response theory[12,13] predicts that in the linear small field limit,

$$\lim_{t\to\infty}\langle J_x(t)\rangle=-\int_0^t \mathrm{d}s\ \chi(t-s)\ F(s) \tag{19}$$

where the susceptibility, χ, is

$$\chi(t)=\frac{-V}{kT}\langle J_x(t)J_x(0)\rangle \tag{20}$$

Using Eq. (18) for $J_x(0)$ and $J_x(t)$, Eq. (20) can be written in terms of the velocity auto-correlation function in the Green-Kubo equatuion, Eq. (6):

$$\chi(t)=\frac{-N^2}{(N-1)VkT}\langle v_{xi}(t)\,v_{xi}(0)\rangle \tag{21}$$

The required equation can be easily obtained from Eqs. (6) and (21):

$$D_s=\frac{(N-1)VkT}{N^2}\lim_{F\to 0}\left[\lim_{t\to\infty}\frac{\langle J_x(t)\rangle}{F}\right] \tag{22}$$

To calculate the self-diffusion coefficient D_s, we apply a condtant color field F, calculate the steady state color current J, and use the above equation.

The equations of translational motion for the center of mass are given by

$$\dot{r}_i=p_i/m \tag{23}$$

$$\dot{p}_{xi}=F_{xi}+c_iF-\alpha_t p_{xi} \tag{24a}$$

$$\dot{p}_{yi}=F_{yi}-\alpha_t p_{yi} \tag{24b}$$

$$\dot{p}_{zi}=F_{zi}-\alpha_t p_{zi} \tag{24c}$$

where the external field is applied to only the x-direction and α_t as a parameter from the translational temperatue constraint. The derivation of the terms containing α_t in the equations of motion is obtained using Gauss's principle of least contraint.[4,7] The constant translational temperature constraint requires that

$$\frac{1}{2m}\sum_{i=1}^{N} p_i^2=\frac{3NkT}{2} \tag{25}$$

The parameter can be identified explicitly by multiplying the equations of motion (24) by p_{xi}, p_{yi}, and p_{zi} and summing over all particles

$$\frac{d}{\mathrm{d}t}\left[\frac{1}{2m}\sum_i p_i^2\right]=\frac{1}{m}\sum_i p_i\cdot\dot{p}_i=\frac{d}{\mathrm{d}t}\ \frac{3nkT}{2}$$

$$=0=\sum_i p_i\cdot F_i+F\sum_i\ c_i p_{xi}-\alpha_t\ \sum_i p_i\cdot p_i$$

Thus the parameter α_t is function of time which depend upon the particle colours, velocities, and forces.

$$\alpha_t=\left[\sum_i p_i\cdot F_i+F\sum_i\ c_i p_{xi}\right]/\ \sum_i p_i\cdot p_i \tag{26}$$

The equations of rotational motion about the center of mass for molecular fluids are derived using quaternions follows[14,15]

$$L_i=T_i-\alpha_r L_i \tag{27}$$

$$L_i^b=A_i\ L_i \tag{28}$$

$$\omega_{ik}^b=L_{ik}/I_k,\ k=x,\ y,\ z \tag{29}$$

$$\begin{bmatrix}\dot{q}_{i1}\\ \dot{q}_{i2}\\ \dot{q}_{i3}\\ \dot{q}_{i4}\end{bmatrix}=\frac{1}{2}\begin{bmatrix}-q_{i3} & -q_{i4} & q_{i2} & q_{i1}\\ q_{i4} & -q_{i3} & -q_{i1} & q_{i2}\\ q_{i1} & q_{i2} & q_{i4} & q_{i3}\\ -q_{i2} & q_{i1} & -q_{i3} & q_{i4}\end{bmatrix}\begin{bmatrix}\omega_{ix}^b\\ \omega_{iy}^b\\ \omega_{iz}^b\\ 0\end{bmatrix} \tag{30}$$

where L_i is the angular momentum of molecule i and T_i is the torque on molecule i in the laboratory frame, L_i^b and ω_i^b are, respectively, the angular momentum and angular velocities of molecule i in its principal axis frame, A_i is the

rotation matrix which transforms vectors from the laboratory to principal axis frame of molecule i, I_k is the principal axis moment of inertia of each molecule, and the q_{ik}, $k=1$, 2, 3, 4 are the quaternion parameters related to the Euler angles describing the orientation of molecule i in space. By the similar derivation for the constant translational temperature constraint parameter with the constant rotational constraint

$$\frac{1}{2}\sum_i\sum_k I_k\omega_{ik}^{p2}=\frac{3NkT}{2} \tag{31}$$

the parameter α_r is given by

$$\alpha_r=\sum_i\sum_k \omega_{ik}^p\ T_{ik}^p \Big/ \sum_i\sum_k I_k\omega_{ik}^{p2} \tag{32}$$

The Sllod Algorithm for Shear Viscosity. Among many NEMD methods developed for calculating the shear viscosity the most efficient technique appears to be the sllod algorithm,[2,3] a standard method using homogeneous Lees-Edwards 'sliding brick' boundary conditions.[16] This algorithm sets up a steady state planar Couette flow with the two plates moving in opposite x directions located at $y=\pm\infty$ so that the streaming velocity has a non-zero component in the x direction $du_x/dy=\gamma$ where γ is the constant strain rate.

The linear response theory[12,13] may be applied to the equation of motion in the linear small strain rate γ,

$$\langle P_{xy}(t)\rangle=-\lim_{t\to\infty}\int_0^t ds\ \chi(t-s)\ \gamma(s) \tag{33}$$

where P_{xy} is given by Eq. (10) and

$$\chi(t)=\frac{-V}{kT}\ \langle P_{xy}(t)\ P_{xy}(0)\rangle \tag{34}$$

is the susceptibility. Taking the integration over time t in Eq. (34), $\chi(t)$ becomes equal to the integrand of the Green-Kubo relation for the shear viscosity, Eq. (8). In the limit of $t\to\infty$ in Eq. (33) with a constant strain rate γ (s), combining with the integrated form of Eq. (34) the shear viscosity can be given by

$$\eta=\lim_{\gamma\to 0}\left[\lim_{t\to\infty}\frac{\langle P_{xy}(t)\rangle}{\gamma}\right] \tag{35}$$

Following Evans and Morriss,[2,3] the equations of translational motion for the center of mass in a molecular fluid are given by:

$$\dot{x}_i=p_{xi}/m+y_i\gamma \tag{36a}$$

$$\dot{y}_i=p_{yi}/m \tag{36b}$$

$$\dot{z}_i=p_{zi}/m \tag{36c}$$

$$\dot{p}_{xi}=F_{xi}-p_{xi}\gamma-\alpha_t p_{xi} \tag{37a}$$

$$\dot{p}_{yi}=F_{yi}-\alpha_t p_{yi} \tag{37b}$$

$$\dot{p}_{zi}=F_{zi}-\alpha_t p_{zi} \tag{37c}$$

The constant translational temperature constraint parameter α_t can be derived in the same process for Eq. (26) under the same requirement, Eq. (25),

$$\alpha_t=\sum_i\left[(p_i\cdot F_i-p_i p_i:\nabla u)\right]/\sum_i p_i^2 \tag{38}$$

The equations of rotational motion about the center of mass for molecular fluids and the constant rotational temperature constraint parameter are given as the same equations, Eq. (27)-(32), as in Sec. III. (1).

The Evans Algorithm for Thermal Conductivity. One of the most difficult thermal transport coefficients to calculate has proven to be the thermal conductivity. The most efficient presently known algorithm is developed by Evans.[5,6] This technique is synthetic in that a fictitious vector field replaces a temperature gradient as the force driving a heat flux and is homogeneous, unlike real heat flow, with no temperature or density gradients being present.

In the linear small external field F_z, the ensemble average of corresponding thermodynamic heat flux at time t is given by

$$\langle J_{Qz}(t)\rangle=-\lim_{Fz\to 0}\int_0^t ds\ \chi(t-s)\ F_z(s) \tag{39}$$

where the susceptibility, χ, is

$$\chi(t)=\frac{-V}{kT}\langle J_{Qz}(t)\ J_{Qz}(0)\rangle \tag{41}$$

Integrating over time t in Eq. (39) and using Eq. (12), we obtain

$$\lambda=-\frac{1}{T}\int_0^\infty dt\ \chi(t) \tag{41}$$

Further using Eq. (31) in the limit of $t\to\infty$ with constant $F_z(s)$, the thermal conductivity is derived as

$$\lambda=\frac{1}{T}\lim_{Fz\to 0}\left[\lim_{t\to\infty}\frac{\langle J_{Qz}\rangle}{F_z}\right] \tag{42}$$

Consider the equations of motion for the center of mass:

$$\dot{r}_i=p_i/m \tag{43}$$

$$\dot{p}_i=F_i+(E_i-E)F(t)+\frac{1}{2}\sum_j F_{ij}r_{ij}\cdot F(t)$$

$$-\frac{1}{2N}\sum_{j,k}F_{jk}r_{jk}\cdot F(t)-\alpha_t p_i \tag{44}$$

where E_i and $\bar{E}$ are, respectively, the instantaneous energy of molecule i, Eq. (16), and the average energy of the system, the constant translational temperature constraint parameter, α_t, is

$$\alpha_t=\frac{\sum_i\left[F_i+(E_i-\bar{E})F(t)+\frac{1}{2}\sum_j F_{ij}r_{ij}F(t)-\frac{1}{2N}\sum_{j,k}F_{jk}r_{jk}\cdot F(t)\right]\cdot p_i}{\sum_i p_i\cdot p_i} \tag{45}$$

and F_{ij} is the force on particle i due to j. The equations of rotational motion and the parameter α_r are again given as the same in Sec. III. (1).

The Details of NEMD Simulation of TIP4P Water. The TIP4P potential for water is used because this potential is a quite reasonable model in comparison to diffraction data and thermodynamic aspects for simulations of liquid water at 298.15 K and 1 atm.[17] The water molecule is assumed to be rigid and to interact through a Lennard-Jones potential between the oxygen atoms and Coulombic potentials between positive charges located at the hydrogen atoms and one negatively charged site on a point M located on the HOH bisector 0.15 A form the oxygen to the hydrogens. The general

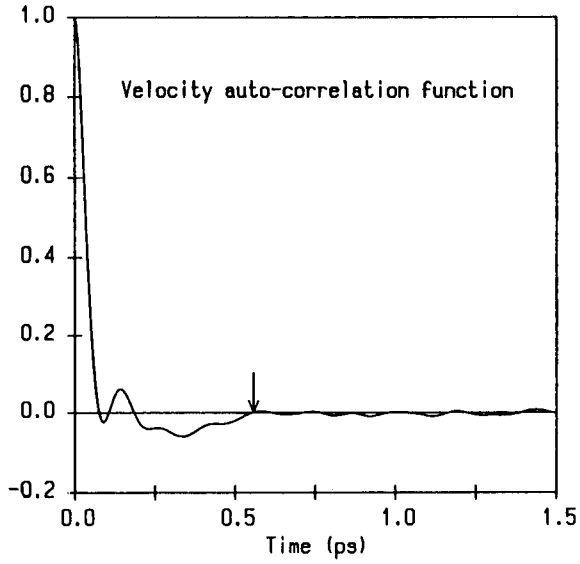

Figure 1. Normalized velocity auto-correlation function for water at 298.15 K and 1 atm. The arrow indicates the point at which the correlation is assumed to be zero.

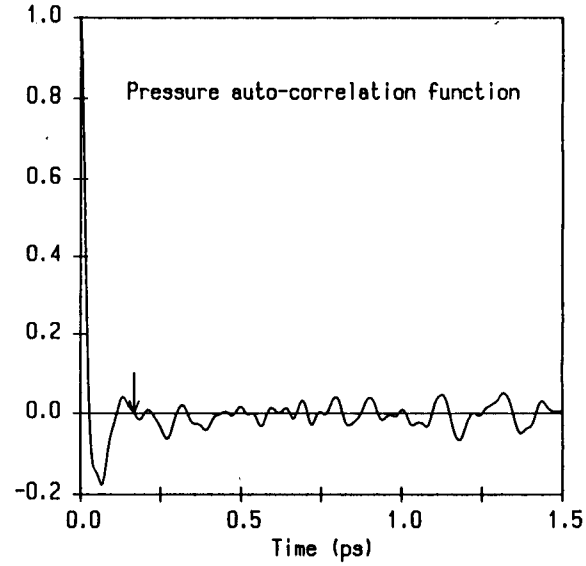

Figure 2. Normalized pressure auto-correlation function for water. The legend is the same as that of Figure 1.

form of intermolecular potential is given by

$$u(r_i, r_j)=T(r_{ij}^{00})\left[\sum_k^{on\,i}\sum_l^{on\,j}(q_i^k\, q_j^l\, e^2/r_{ij}^{kl})\right.$$
$$\left.+A\,(r_{ij}^{oo})^{-12}-C(r_{ij}^{oo})^{-6}\right] \quad (46)$$

where

$$T(r)=\begin{cases}1, & r<r_t\\ 1-(r_c-r_t)^{-3}(r-r_t)^2(3r_c-r_t-2r), & r_t\le r<r_c\\ 0, & r\ge r_c\end{cases} \quad (47)$$

is the switch function for smoothly ending potential fucntion to zero, $r_t=0.95\ r_c$, and r_c is the cutoff radius and is chosen to be 8.5 A, and where q_i is the charge on site k of molecule i in units of e, r_{ij}^{oo} is the distance between the centers of the oxygen atoms in two molecules, and r_{ij}^{kl} the distance between site k of molecule i and site l of molecule j. The Lennard-Jones parameters are $A=600{,}000$ kcal A^{12}/mol and $C=610$ kcal A^6/mol. Two positive charges of 0.52 e are on the hydrogens and the negative charge of -1.04 e on the M site. The OH bond length (0.9752 A) and *HOH* angle (104.52°) are fixed at the experimental values for the water monomer.[18] The preliminary NVT MD simulation of 216 water molecules was started in the cubic box of length $L=18.645$ A of which the density is equal to 0.9969 g/cm^3 at 298.15° K and 1 atm. The equations of motion are solved using a fifth-order predictor-corrector Gear integration[19] with a time step of 2×10^{-15} second.

Results and Discussion

The velocity, pressure, and heat flux auto-correlation functions obtained from the EMD simulations are drawn in Figures 1-3. The curve in Figure 1 is averaged over 700 sets of individual curves and the curves in Figures 2 and 3 are over 1700 sets as in our previous study.[1] The thermal transport coefficients, of water at 298.15 K and 1 atm, calculated by integrating these correlation functions over $t=0$ to $t=1.5$ ps using Simpson's rule[20] are given in column (1) of Table 1. The calculated self-diffusion coefficient is in good agreement with Neumann's TIP4P water simualtion result[21] (2.8×10^{-5} cm^2/sec at 293 K) and another TIP4P result[22] (2.95×10^{-5} cm^2/sec at 298 K). But the comparison of the calculated shear viscosity and thermal conductivity with experimental results given in column (3) of Table 1 shows very poor agreements.

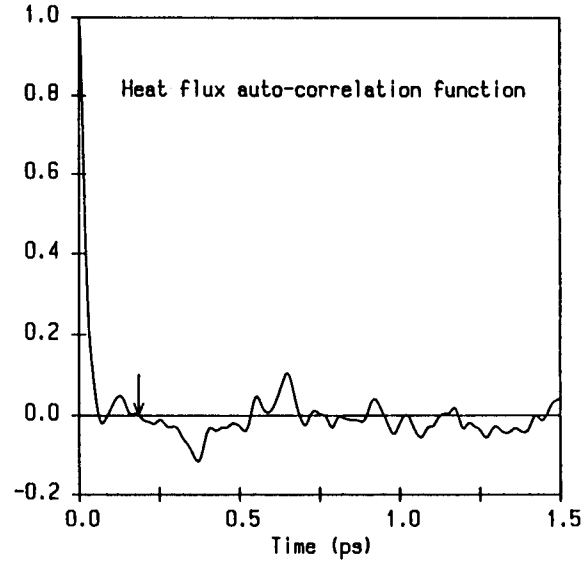

Figure 3. Normalized heat flux auto-correlation function for water. The legend is the same as that of Figure 1.

The failure of Green-Kubo relations for the shear viscosity and thermal conductivity of liquid water is rather difficult to be explained. The upper integration limit $t=\infty$ in Eqs. (6), (8), and (12) cam be replaced by a finite value when the correlation between $x(0)$ and $x(t)$ becomes zero where $x=v_x$, P_{xy}, and J_{Qx}. For the well-behaved curve, as shown in Figure 1, which is not oscillating and decaying rapidly, the time point of zero correlation is easily determined. But

Table 1. Comparison of The Results Obtained from The Green-Kubo Relations for The Thermal Coefficients of Liquid Water at 298.15 K and 1 atm other MD and NEMD Simulation Results and Experimental Results

Transport properties	Gerrn-Kubo (1)	Gerrn-Kubo (2)	Experimental results (3)	Other MD and NEMD results (4)
Self-diffusion coefficients (10^{-5}cm^2/sce)	3.10	3.24	–	2.8[a] (293 K) 2.95[b]
Viscosity (cp)	0.0752	0.874	0.8904[c] (298.15 K)	0.428[d] (303.15 K)
Thermal conductivity (milli·watt/cm·K)	0.713	3.87	6.098[c] (300 K)	–

[a]Ref. 21, [b]Ref. 22, [c]Ref. 29, [d]Ref. 28, [e]Ref. 30.

in the other case, as shown in Figures 2 and 3, it is difficult to determine those time points. Plausible points of zero correlation are determined roughly and indicated as arrows in Figures 1-3 and the results of the integration over zero to these points are given in column (2) of Table 1. The agreements with the experimental data are much better than those of column (1). In Figure 1, the correlation after the arrow point is very small but there is still a recognizable difference of the self-diffusion coefficients between column (1) and (2) which may mean the need of more runs to be averaged. On the other hand, the correlations after the arrow points in Figures 2 and 3 show big fluctuation which reflects huge differences of the shear viscosities and thermal conductivities between column (1) and (2).

From the above discussion, the failure of Green-Kubo relations for the shear viscosity and thermal conductivity of liquid water is closely related to the failure of obtaining well-behaved pressure and heat flux auto-correlation functions of liquid water. We may analyze this problem in two ways: the comparison of the auto-correlation functions of liquid water with those of liquid argon which is modeled by a simple Lennard-Jones potential and the exception for the velocity auto-correlation function of liquid water.

First of all, we may interprete the non-decaying correlation of pressure and heat flux of liquid water as due to the complexity of the model potential (TIP4P) which is characterized by the Coulomb potentials between charges on water molecules. But it is difficult to understand how the potential affects the equations of pressure tensor P_{xy} and heat flux J_{Qx}, Eqs. (10) and (14). In order to clarify this effect we may run a computer simulation with much bigger capacity to record all the correlation of each water molecule over long times for the purpose of later analysis. It is possible that sufficient runs of simulations and more statistical precision in averaging of the correlation curves overcomes this problem. Another possibility is the size of simulation box. If one wishes to calculate a time-correlation function over a time span t, then one must ensure that the system simulated is sufficiently large for a sound wave not to be able to traverse the system in a time less than t.[23]

The velocity auto-correlation functions of both liqud argon[1]

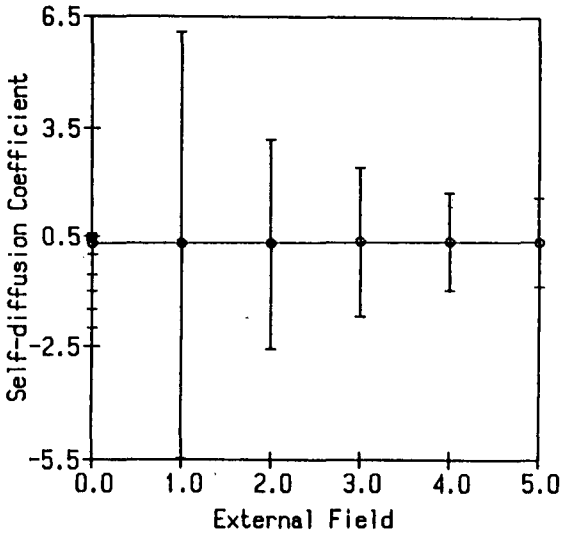

Figure 4. NEMD simulation results for self-diffusion coefficient, in the unit of 10^{-6} cm^2/sec, of water at 298.15 K and 1 atm as a function of external field (g · nm/mole · ps^2). The circle at zero external field is obtained least squares fit of the results to a straight line and ■ is the EMD result. The error bars indicate the standard deviation.

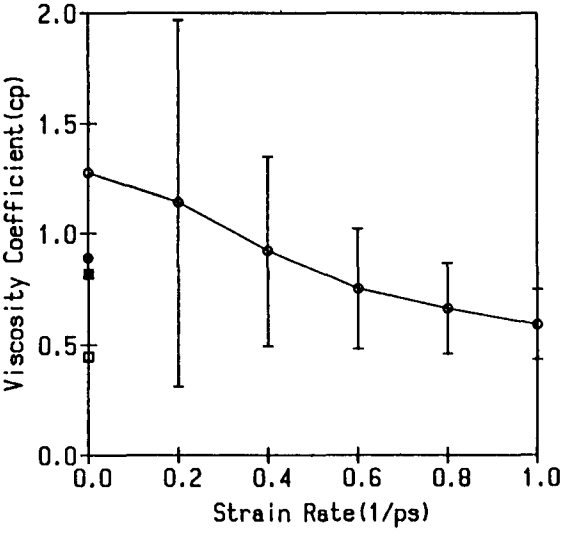

Figure 5. NEMD simulation results for shear viscosity, in the unit of cp, of water at 298.15 K and 1 atm as a function of strain rate (ps^{-1}). The white circle at zero external field is obtained by Lagrange extrapolation[24] and the black circle indicates an experimental result. □ and ■ represent, respectively, the NEMD result for shear viscosity of water by Cummings and Varner[28] and an experimental result at 303.15 K and 1 atm. The error bars indicate the standrd deviation.

and liquid water show well-behaved smooth curves in contrast to the pressure and heat flux auto-correlation functions of liquid water. The first possibility to explain this result may be due to the property of the center-of-mass velocity of molecule. Since the forces on atoms in each molecule is directly calculated from the model potential, but the force on the center-of-mass is calculated by summing of the forces on atoms and the center-of-mass velocity is calculated by

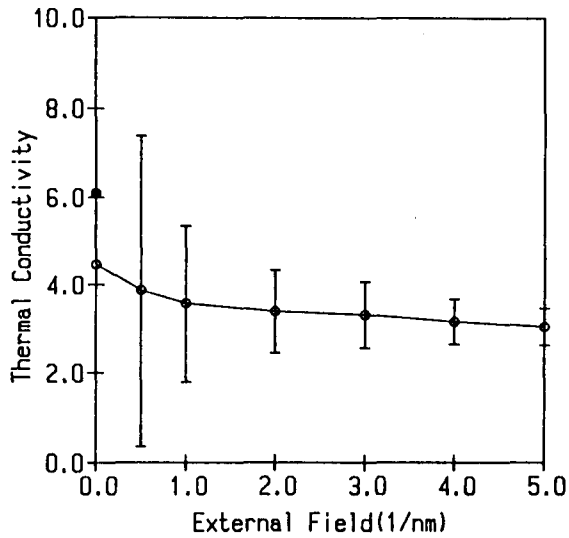

Figure 6. NEMD simulation results for thermal conductivity, in the unit of milli · watt/cm · K, of water at 298.15 K and 1 atm as a function of external field (nm^{-1}). The white circle at zero external field is obtained by Lagrange extrapolation[24] and the black circle indicates an experimental result at 300 K and 1 atm. The error bars indicate the standard deviation.

Table 2. NEMD simulation results for the self-diffusion coefficient (D_s), shear viscosity (η), and thermal conductivity (λ) of liquid water at 298.15 K and 1 atm. D_s at zero external field is obtained by least squares fit of the results to a straight line, and η and λ are obtained by Lagrange extrapolation at zero external field[24]

External field ($g \cdot nm/mole \cdot ps^2$)	5.0	4.0	3.0	2.0	1.0	0.0
Self-diffusion coefficients (10^{-5} cm^2/sec)	3.46 ± 12.2	3.57 ± 13.4	3.59 ± 20.5	3.16 ± 28.8	3.14 ± 57.8	3.07
Strain rate(ps^{-1})	1.0	0.8	0.6	0.4	0.2	0.0
Shear viscosity (cp)	0.592 ± 0.156	0.663 ± 0.202	0.752 ± 0.269	0.922 ± 0.427	1.141 ± 0.827	1.277

External field (nm^{-1})	5.0	4.0	3.0	2.0	1.0	0.5	0.0
Thermal conductivity (milli · watt/cm · K)	3.04 ± 0.417	3.16 ± 0.510	3.31 ± 0.750	3.39 ± 0.941	3.57 ± 1.78	3.87 ± 3.52	4.47

time integration of the force, the velocity auto-correlation function of liquid water may not be related to the complexity of model potential as discussed in the above paragraph. Rather the rotational velocity auto-correlation function liquid water may show a bad-behaved curve. The second is that the average $\langle \cdots \rangle$ in Eq. (6) would be computed for each of the N (=216) molecules in the simulation and this gives a greater statistical precision to the averaged velocity auto-correlation function.

The results of non-equilibrium molecular dynamics (NEMD) simulations for the self-diffusion coefficient, shear viscosity, and thermal conductivity of water at 298.15°K and 1 atm shown in Figures 4-6 and in Table 2. Each NEMD simulation result is averaged over 20,000 time steps after simulation runs of 20,000 time steps to reach a steady state. The self-diffusion coefficient at zero external field is obtained by least squares fit of the non-zero external field results to a straight line, and the shear viscosity and the thermal conductivity are obtained by Lagrange extrapolation[24] at zero external field.

Figure 4 shows the self-diffusion coefficients as a function of external field. The final result at zero external field shows a good agreement with that from obtained from the EMD (Green-Kubo relation) result. Unfortunately there is no experimental data for the self-diffusion coefficient of liquid water. In this study for the calculation of self-diffusion coefficient, we employed Hamiltonian algorithm (Sec. III. (1)) only. Evans and coworkers[4] used Gaussian algorithm in addition to this method and reported that these two non-equilibrium methods are self-consistent within the statistical uncertainities.

Figure 5 shows the NEMD result for shear viscosity of water. It appears that as the strain rate is decreased the shear viscosity increases but it does not seem that the shear viscosity shows the square-root behaviour, as Cummings and Varner expected in their NEMD results.[25-28] Comparing with the experimental value (●), the zero strain rate extrapolated shear viscosity is overestimated by 43%. Other NEMD and experimental result[28] at 303.15 K and 1 atm are also shown in the figure.

In Figure 6 we show the NEMD result for the thermal conductivity of liquid water. As the external field decreases the thermal conductivity is increased very slowly and becomes steep near zero external field. But it is reported that for the thermal conducitivity of a Lennard-Jones fluid at the triple point is decreased almost linearly with decreasing external field.[5] The zero external field extrapolated thermal conductivity is underestimated by 27% compared to the experimental result at 300 K and 1 atm (●).

Concluding Remarks

In this study, we purpose to develope the non-equilibrium molecular dynamics (NEMD) technique to determine the thermal transport coefficients of liquid water at 298.15°K and 1 atm, by using a well-developed potential model for the interactions between the water molecules at the microscopic level. The results obtained from the equilibrium molecular dynamics simulations of TIP4P water model imply the failure of obtaining well-behaved time-correlation functions except the velocity auto-correlation function. The reason for the failure is not clear from the present study. On the other hand, the results of the NEMD simulations of the same model give an agreement with experimental data within approximately 30~40% errors. Even though the uncertainity is rather not negligible, based on this work we may conclude that application of NEMD technique to other dense liquids is promised with well-developed model potentials. In this sense the present study may be considered as a first step towards

the determination of thermal transport coefficients of various aqueous solutions. Further study should assess the analysis of bad-behaved time-correlation functions of molecular liquids.

Acknowledgement. The authors acknowledge the Korea Research Foundation through Non Directed Research Fund, 1989. The authors thank to the Computer Centers at Kyungsung University for the access to the MV/20000 system and at Pusan National University for the access to the Cyber 803 and Cyber 932.

References

1. C. B. Moon, G. G. Moon, and S. H. Lee, *Bull. Kor. Chem. Soc.*, **12**, 309 (1991).
2. D. J. Evans and G. P. Morris, *Phys. Rev.*, **A30**, 1528 (1984).
3. D. J. Evans and G. P. Morris, *Comput. Phys.*, **1**, 297 (1984).
4. D. J. Evans, W. G. Hoover, B. H. Failor, B. Moran, and A. J. C. Ladd, *Phys. Rev.*, **A28**, 1016 (1983).
5. D. J. Evans, *Phys. Lett.*, **A91**, 457 (1982).
6. D. J. Evans, *Phys. Rev.*, **A34**, 1449 (1986).
7. K. F. Gauss, *J. Reine Angew. Math.*, **IV**, 232 (1829).
8. J. R. Rustad, D. A. Yuen, and F. J. Spera, *J. Chem. Phys.*, **91**, 3662 (1989).
9. (a) F. H. Stillinger and T. A. Weber, *J. Phys. Chem.*, **91**, 4899 (1987); (b) *ibid, Phys. Rev.*, **B31**, 5262 (1985).
10. F. O. Raineri, M. D. Wood, and H. L. Friedman, *J. Chem. Phys.* **92**, 649 (1990).
11. (a) M. S. Green, *J. Chem. Phys.*, **19**, 249 (1951); (b) *ibid*, **20**, 1281 (1952); (c) *ibid* **22**, 398 (1954); (d) R. Kubo, *J. Phys. Soc. Japan* **12**, 570 (1957).
12. G. Ciccotti, G. Jacucci. and I. R. McDonald, *J. Stat. Phys.* **21**, 1 (1979).
13. G. P. Morriss and D. J. Evans, *Molec. Phys.*, **54**, 135 (1985).
14. D. J. Evans, *Molec. Phys.*, **34**, 317 (1977).
15. D. J. Evans and S. Murad, *Molec. Phys.*, **34**, 327 (1977).
16. A. W. Lees and S. F. Edwards, *J. Phys.*, **C5**, 1921 (1972).
17. (a) W. L. Jorgensen, J. Chandrasekhar, J. D. Madura, R. W. Impey and M. L. Klein, *J. Chem. Phys.*, **79**, 926 (1983); (b) W. L. Jorgensen and J. D. Madura, *Molec. Phys.*, **56**, 1381 (1985).
18. (a) G. S. Kell, *J. Chem. Eng. Data* **20**, 97 (1975); (b) N. E. Dorsey, "Properties of Ordinary Water Substances" (Rheinhold, New York, 1940); (c) R. Mills, *J. Phys. Chem.*, **77**, 685 (1974).
19. W. C. Gear, 'Numerical Initial Value Problems in Ordinary Differential Equations' (McGraw-Hill, New York, 1965).
20. S. H. Kuo, "Computer Applications of Numerical Methods" (Addison-Wesley, Philippines, 1972), p. 280.
21. M. Neumann, *J. Chem. Phys.*, **85**, 1567 (1986).
22. S. H. Lee and P. J. Rossky, in "Proceedings of the 10th Korean Scientists and Engineers Conference" (Inchen, Korea 1987), Physical science part, p. 150.
23. W. W. Wood, "Fundamental Problems in Statistical Mechanics III" p. 331 ed. E. G. D. Cohen (1975).
24. S. H. Kuo, "Computer Applications of Numerical Methods" (Addison-Wesley, Philippines, 1972), p. 244.
25. A. D. Simmons and P. T. Cummings, *Chem. Phys. Lett.*, **129**, 92 (1986).
26. (a) P. T. Cummings and G. P. Morris, *J. Phys. F: Met. Phys.*, **17**, 592 (1987); (b) P. T. Cummings and G. P. Morris, *J. Phys. F: Met. Phys.*, **18**, 1439 (1988).
27. B. Y. Wang and P. T. Cummings, *Inter. J. Thermo.*, **10**, 929 (1989).
28. P. T. Cummings and T. L. Varner, *J. Chem. Phys.*, **89**, 6391 (1988).
29. "CRC Handbook of Chemistry and Physics" 70th ed. (CRC Press. Inc., Boca Raton, 1989), F-40.
30. *J. Phys. Chem. Ref. Data*, **15**, 1080 (1986).

Characterization of Spherical Particles by Light Scattering

Sangwook Park, Jungmoon Sung, and Taihyun Chang*

Department of Chemistry, POSTECH, Pohang 790-600
Division of Organic Materials, RIST, Pohang 790-600. *Received January 30, 1991*

We have studied a characterization method of accurate size of spherical particles by fitting experimental light scattering profile to the rigorous theoretical scattering function. An efficient software has been developed for computation of the theoretical scattering function and regression analysis. A light scattering instrument has been built and the necessary data acquisition and analysis are carried out by use of a personal computer with an emphasis on the reduction of analysis and time aiming that this study will be extended toward a development of a practical particle sizing apparatus. The performance of the instrument and the software has been evaluated with latex spheres and found to be satisfactory.

Introduction

Particles exist in various forms, solid (powder), liquid (suspension or emulsion), gas (aerosol), and play an indispensable role in a number of important industrial processes. They exhibit unique properties due to their high surface area to